06

Brominated porous carbon material for terahertz radiation shielding

© K.I. Baskakova,[1] O.V. Sedelnikova,[1] A.D. Nishchakova,[1] E.V. Shlyakhova,[1] A.D. Fedorenko,[1] A.G. Paddubskaya,[2] N.I. Valynets,[2] L.G. Bulusheva,[1] Y.V. Fedoseeva,[1] A.V. Okotrub[1]

[1]Nikolaev Institute of Inorganic Chemistry, Siberian Branch, Russian Academy of Sciences,
630090 Novosibirsk, Russia
[2]Institute for Nuclear Problems, Belarusian State University,
220030 Minsk, Belarus
e-mail: fedoseeva@niic.nsc.ru

Received September 26, 2024
Revised September 26, 2024
Accepted September 26, 2024

Porous carbon material obtained by thermal decomposition of acetonitrile on template CaO particles was brominated in saturated bromine vapor at room temperature. This modification led to the addition of 3 at% bromine and increased its electrical conductivity by 3.2 times. Polymer films were made from polystyrene with the addition of starting or brominated porous carbon materials at different concentrations (from 1 to 10 wt%) to study the effect of bromination on the electromagnetic properties of composite materials in the frequency range from 0.1 to 1.3 THz. An increase in the shielding of terahertz radiation with increasing filler concentration has been shown. At low contents, the shielding efficiency of the composites filled with brominated porous carbon material increased by several times compared with the samples filled with the initial one that was associated with the modification of the electronic structure of porous carbon material during the bromination procedure.

Keywords: porous carbon material, bromination, polymer composite, shielding of terahertz electromagnetic radiation.

DOI: 10.61011/TP.2025.02.60814.295-24

Introduction

Great attention to porous carbon materials (PCM) is due to their unique physical and chemical properties and wide application range [1]. These materials are characterized by high specific surface area, developed porous structure, good electrical conductivity and chemical stability, and accessibility and scalability of the fabrication techniques. Therefore PCM are used in such areas as power engineering [2–4], gas and impurity adsorption [5], catalysis [6,7].

PCM consist of curved fold graphene layers, which makes them similar to laminated graphene-like materials. Unlike the ideal flat two-dimensional graphene, PCM has a three-dimensional structure without long-range order [8]. Structural features and high porosity of carbon materials make them similar to with carbon nanohorns (CNH) [9–11], carbon foams [12–16] and aerogels [17]. These materials effectively reduce the power of transmitted electromagnetic radiation. This is achieved through a combination of intrinsic absorption by graphene-like particles and multiple reflections of electromagnetic waves within the porous structure. However, PCM are currently hardly used as fillers for electromagnetic applications.

Addition of functional groups modifies the electronic structure of carbon particles, which may have a positive effect on the electromagnetic properties of polymer materials containing such filler. Graphene-like materials easily react with halogens. Fluorine and chlorine attach to the basal plane of carbon materials reducing of their electrical conductivity due to the failure of the conductive π-system. Less reactive bromine primarily reacts with carbon atoms placed at the edges of graphene fragments and vacancy defects. Thus, C−Br bond is in the graphene plane [18]. Furthermore, bromine molecules can be embedded between layers and into pores between carbon nanoparticles causing the transfer of electron density from the carbon material to bromine [19]. It has been shown before that bromination of graphite particles and single-layer nanotubes improves their electrical conductivity [20,21]. Therefore, the objective of the study was to explore the PCM bromination effect on electrical conductivity and the electromagnetic shielding efficiency when PCM is used as a filler for polymer composite materials. The bromination effect was studied on a porous nitrogen-containing carbon material made from acetonitrile using a previously developed procedure [22].

1. Materials and methods

1.1. Materials

1.1.1. Porous carbon material synthesis procedure

Iron-doped calcium tartrate ($Ca_{0.97}Fe_{0.03}C_4H_4O_6$) was prepared by mixing a solution containing calcium chloride ($CaCl_2$) and iron II sulfate ($FeSO_4$) with a freshly prepared sodium tartrate aqueous solution ($Na_2C_4H_4O_6$) in nitrogen atmosphere. Accurately weighed $CaCl_2$ and $FeSO_4$ were taken in proportions necessary to prepare calcium salt containing 3 at% iron. The obtained precipitate was filtered

through a paper filter to pH-neutral wash water and dried in air. Nitrogen-containing PCM was synthesized by chemical vapor deposition in a horizontal tubular quartz reactor at 650°C. 1 g of $Ca_{0.97}Fe_{0.03}C_4H_4O_6$ powder in a ceramic crucible was placed on the reactor periphery that was not subjected to heating when the external heating element was activated. The reactor was evacuated using a prevacuum pump. Saturated acetonitrile vapor (CH_3CN) was supplied to the reactor during continuous evacuation and evaporated from the liquid surface at room temperature. Then the crucible was moved to the reactor hot zone using a handle. Thermal decomposition of the salt, acetonitrile vapor precipitation and pyrolysis took place simultaneously during 40 min. $Ca_{0.97}Fe_{0.03}C_4H_4O_6$ was a precursor for the templated nanoparticles, and CH_3CN was a carbon and nitrogen source for PCM formation. The reaction product was cleaned to remove the templated CaO nanoparticles in aqueous solution of hydrochloric acid (~ 6 M), rinsed repeatedly in distilled water to neutral pH, filtered through a membrane filter and dried at 100°C during 3 h.

1.1.2. Bromination of the porous carbon material

PCM bromination was conducted in saturated molecular bromine vapor (Br_2) using a procedure for preparation of bromine-intercalated graphite compounds [23]. For this, liquid bromine was poured on the bottom of a polytetrafluoroethylene (PTFE) reactor with an accurately weighed PCM sample in a perforated PTFE insert placed above the liquid bromine. The reactor was sealed and held at room temperature during four days. Due to bromine binding, the sample weight increases. As was shown above, the main growth of weight during the bromination of carbon fibers takes place within the first 48 h [24]. After bromination, the sample weight remains constant during longer interaction with Br_2. Brominated carbon materials removed from the reactor (from the saturated Br_2 vapor atmosphere) gradually loose their loosely-bound adsorbate. According to the isotherms of bromine adsorption-desorption on pyrolytic graphite, about 30% of the total bromine bound in saturated Br_2 vapor is entrapped in the graphite [23]. For effective removal of loosely-bound bromine molecules, the PCM bromination product was nitrogen purged at room temperature until the loss of weight was completed (about 24 hours in this case). Thus, the weight growth after bromination was 7%. The prepared material was designated as PCM-Br.

1.1.3. Composite polymer material fabrication procedure

Polystyrene (PS) with a density of 1.04 g/cm^3 was used as a polymer matrix for composite materials. A procedure for fabrication of PS-based composite materials filled with carbon nanomaterials is described in our previous works [25–27]. An accurately weighed carbon material was added to 20 ml of chloroform ($CHCl_3$) and treated using an ultrasonic (US) disperser (UZTA-0,4/22-OM „Volna“) with an operating power of 120 W during 40 min to obtain a stable suspension. PS was added to the suspension and the US treatment was repeated using the Sonopuls mini20 (Bandelin) during 20 min at 20 W. The prepared homogeneous suspensions were transferred into Petri dishes and held in a hood at room temperature for 24 h. As a result, two series of polymer films were made with PCM or PCM-Br samples used as a filler. Composite polymer samples were designated as PS/PCM and PS/PCM-Br. The content of filler in PS varied from 1 to 10 wt%. As the concentration increased, the color of the samples changed from light-grey to black. Film thickness was uniform throughout the sample, but varied from 70 to 150 μm for different filler content. Polystyrene bromination shall be excluded during the composite material fabrication process because this reaction can only take place in the presence of aromatic ring activators (Lewis acids, N-bromosuccinimide, etc.) [28,29].

1.2. Structural characterization

Sample morphology was examined by scanning electron microscopy (SEM) on a Hitachi S-3400N (Hitachi Ltd.) microscope with an accelerating voltage of 5 kV. Textural properties were tested by low-temperature nitrogen adsorption using the „Sorbi-MS“ (META) laboratory sorptometer at a liquid nitrogen temperature of -196°C. Before the measurements, the samples were preliminary heat treated in nitrogen at 150°C during 1.5 h to remove the occluded air molecules. Extra pure grade nitrogen was used as adsorbate gas, extra pure grade helium was used as carrier. Surface area of the samples was calculated by the Brunauer–Emmett–Teller method. Structural analysis of the samples was carried out by Raman scattering spectroscopy using the LabRAM HR Evolution (Horiba Ltd.) spectrometer with argon laser excitation ($\lambda = 514$ nm, excitation power of 60 mW).

Elemental composition of the carbon material surfaces was measured by X-ray photoelectron spectroscopy (XPS) using a FlexPS system (Specs GmbH) laboratory spectrometer equipped with monochromator and PHOIBOS 150 analyzer. The working chamber pressure was $\sim 10^{-7}$ Pa. Monochromatized Al K_α-radiation (1486.71 eV) was used for spectra excitation. Absolute energy spectra scale was referenced to the graphite maximum position at 284.4 eV. Bond energy measurement error was ± 0.1 eV. Background was subtracted from the experimental curves using the Shirley method [30]. Spectra were approximated by a set of components represented by the product of the Gaussian and Lorentz functions. All XPS spectra were processed and approximated using the CasaXPS software Version 2.3.15. Thermogravimetric analysis (TGA) was performed using a STA 449 F1 Jupiter (NETZSCH Group) thermoanalyzer. Measurements were carried out in open Al_2O_3 crucibles in He atmosphere at a flow rate of 20 ml/min in the

temperature range of 30−1010°C with a heating rate of 10°C/min.

1.3. Measurement of electrophysical properties

DC electrical conductivity σ_{DC} of PCM and PCM-Br powders was measured by a four-contact method using the Source Meter 2400 (Keithly Instruments) calibrator-multimeter in a cylindrical dielectric cell (4 mm in diameter and 9 mm in height). Electrical contacts were made from 0.1 mm copper wire.

THz transmission and reflection spectra of composite materials were recorded using a THz time-domain spectrometer T-SPEC (Ekspla). All measurements were performed at normal incidence. Diameter of the subpicosecond THz beam in the focusing point was about 3 mm. To improve the signal-to-noise ratio, additional averaging over 1024 measurements was performed. Relative transmission and reflection coefficients were measured in the frequency range of 0.1−1.3 THz. Real (ε') and imaginary (ε'') parts of the complex permittivity $\varepsilon = \varepsilon' + i\varepsilon''$ were calculated from the measured transmitted and reflected wave powers in accordance with the procedure described in detail elsewhere [31–33]. The calculated dielectric permittivity data was used to evaluate transmittance (T), reflectance (R) and absorbance (A) for the corresponding 100 μm films.

2. Findings and discussion

2.1. Structure of carbon materials

SEM images of PCM samples (Figure. 1, *a*) and PCM-Br (Figure 1, *b*) demonstrate that materials are a network of entangled thin carbon layers, and have a developed porous surface and large void (pore) volume. Equivalent results were obtained in our previous works for PCM synthesized in similar conditions [34–36]. Bromination of the studied carbon material didn't cause any significant changes in its morphology.

Raman spectra of the PCM and PCM-Br samples demonstrate two wide peaks at 1347 cm^{-1} (band D) and 1590 cm^{-1} (band G) that are typical of sp^2-hybridized carbon materials [37,38] (Figure 2, *a*). Band intensity ratio I_D/I_G is used for qualitative characterization of carbon material defects. $I_D/I_G = 0.8$ calculated for PCM indicates a high content of defects in the hexagonal structure of carbon materials. A wide 2D-peak at 2790 cm^{-1} corresponds to the second order of D-mode, a flat peak tip indicates that the studied materials consist of graphene, graphite and few-layer graphene fragments with different number of layers [37]. The Raman spectrum of PCM-Br has a shape and I_D/I_G compared with the PCM spectrum. The employed bromination technique doesn't damage the PCM carbon layer structure, and bromine binds primarily to the edge carbon atoms. Specific surface area of the initial PCM is 577 ± 25 m^2/g and decreases to 430 ± 21 m^2/g for PCM-Br. Decrease in the specific surface area may be associated with the fact that bromine atoms cover some pores and increase the sample weight.

XPS method was used to examine the composition of the PCM and PCM-Br sample surfaces and chemical states of atoms in them. Carbon is a dominating element in the samples (Figure 2, *b*). Moreover, PCM contains 5 at% nitrogen and 8 at% oxygen. 4 at% nitrogen and 8 at% oxygen were found in PCM-Br. Concentration of these elements remained almost unchanged after bromination. About 3 at% bromine was found in PCM-Br.

To determine chemical state of elements in the samples, chemical shifts of photoelectron core lines were analyzed. A wide profile of the XPS C 1s spectra with the major peak at 284.4 eV indicates that carbon walls consist of sp^2-hybridized carbon atoms that form a graphene-like layer structure (Figure 2, *c*). An intense component at 285.3 eV may be formed by defects, C−H or C−O bonds, a component at 286.8 eV is induced by C=O and C=N bonds, and a component at 288.6 eV is induced by carboxyl groups [39]. After bromination, the profile of C 1s spectra remains almost unchanged. Contribution to the spectrum from covalent C−Br bonds may be expected at 285.3 eV, however, it cannot be distinguished unambiguously due to a low content of bromine and overlapping between this components and the states of defects, C−H and C−O bonds. Analysis of the XPS O 1s spectra confirmed the presence of C−O and C=O bonds in PCM, number of the bonds and proportion remained unchanged after bromination (Figure 2, *d*). Oxygen can be included in hydroxyl, carboxyl, ether and carbonyl groups that were formed on the PCM surface in interaction with air.

XPS N 1s spectrum of PCM identifies thee forms of nitrogen in the sample [4] (Figure 2, *e*). A component at 398.3 eV is generally assigned to two-coordinated (pyridinic) nitrogen that is located at the edges of graphene fragments and has an electronic configuration as that of a pyridine molecule. A component at 401.7 eV is induced by so-called graphitic nitrogen that substituted a carbon atom in the hexagonal graphene grid. The most intense peak at 400.0 eV (its fraction is 62%) corresponds to hydrogenated nitrogen atoms that substitute the edge carbon atoms. These nitrogen atoms and graphitic nitrogen give a part of their electron density to the conjugated graphene π-system, which increases the number of charge carriers and improves graphene's conductivity. Pyridinic nitrogen, on the contrary, is an electron density acceptor. Bromination didn't cause any significant change of the chemical state and relative concentration of nitrogen forms in the carbon material structure. Two chemical states of bromine were identified in the XPS Br 3d spectrum of PCM-Br (Figure 2, *f*): intercalated Br_2 molecules (doublet with the Br $3d_{5/2}$ bond energy 68.1 eV) and bromine covalently bound to carbon (C−Br) (doublet with Br $3d_{5/2}$ bond energy 70.1 eV) [40–42]. The ratio of Br_2 and C−Br in the sample is 2 : 3. As long as bromination was performed in mild conditions without heating and Br_2 dissociation, the degree of bromination is low, and bromine binding to carbon layers is accompanied by the formation of

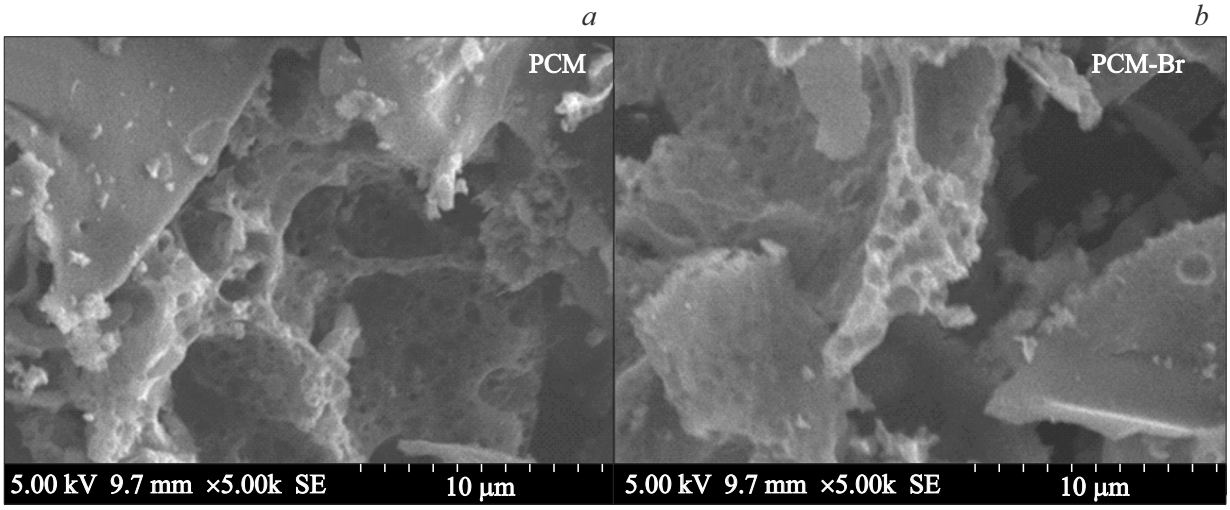

Figure 1. SEM microphotographs of the initial PCM (*a*) and brominated PCM-Br (*b*).

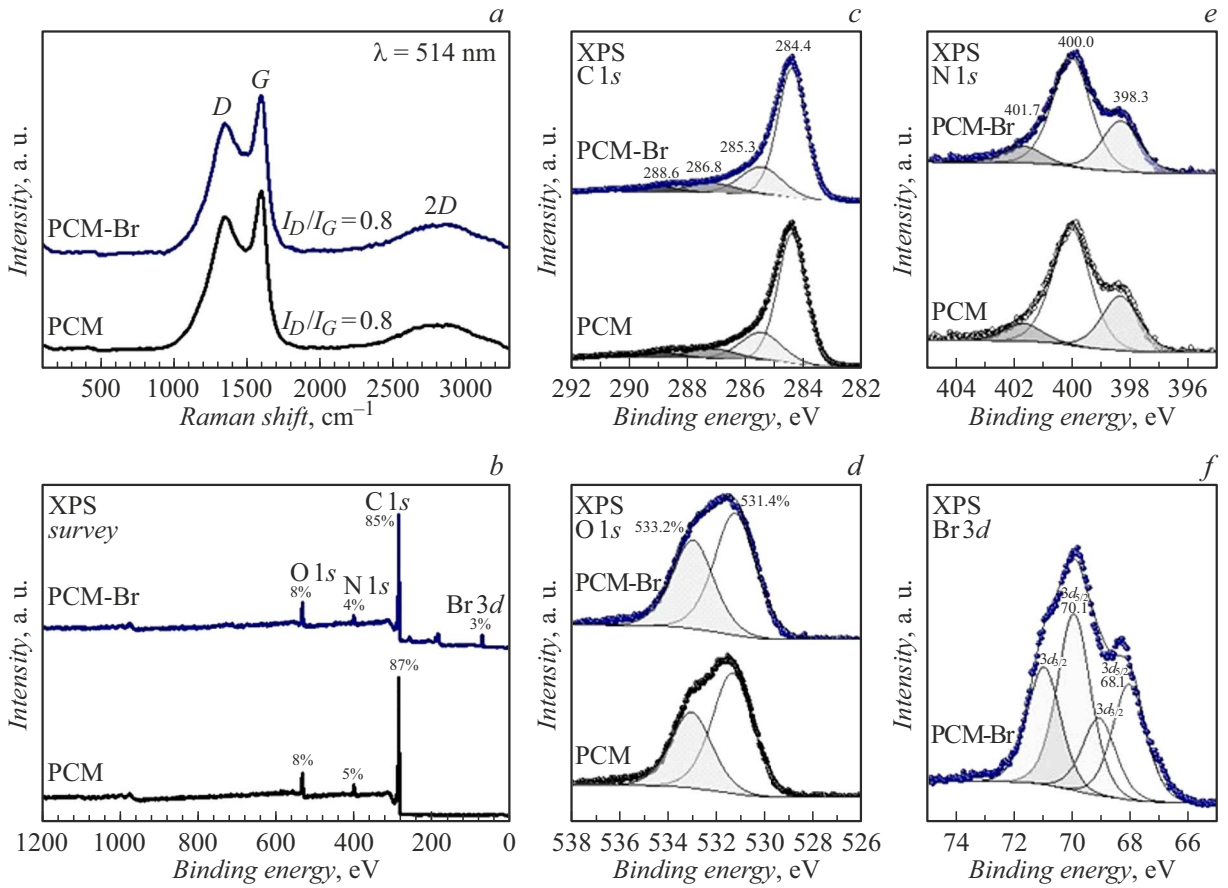

Figure 2. Raman spectra (*a*) and XPS survey spectra (*b*), C 1s (*c*), O 1s (*d*), and N 1s (*e*) spectra of PCM and PCM-Br. XPS Br 3d spectrum of PCM-Br (*f*).

C−Br bonds at the graphene-like area edges and of defect states, which doesn't distrub the delocalized π-system.

Stability of the PCM-Br sample was examined by the TGA method in inert atmosphere. The PCM-Br sample thermogram (Figure 3) is similar to curves described in the literature for brominated carbon fibers [43], which showed that desorption of intercalated bromine may occur in the temperature range of 100−250°C, and covalent C−Br bonds may be broken at 250−650°C. However, desorption of water, nitrogen, oxygen-containing and carbon-containing

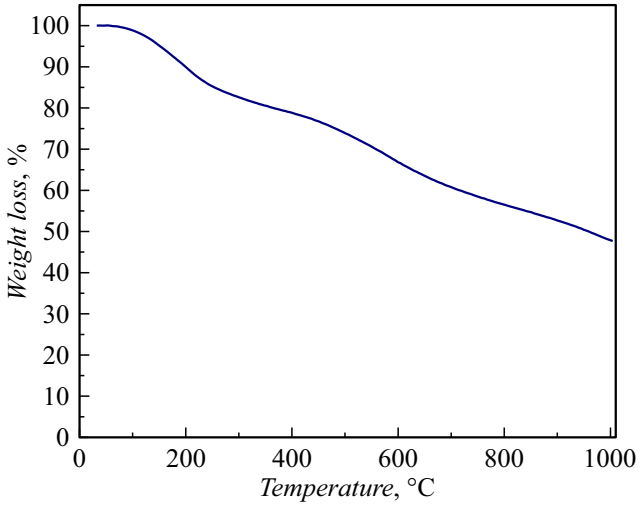

Figure 3. Thermogravimetric curve for the PCM-Br sample.

compounds may occur in this temperature range, which explains the observed high loss of weight (15% at 250°C and 37% at 650°C). PCM-Br has a sufficient thermal stability for various materials science applications, in particular, as a functional additive to polymer matrices.

2.2. Electrical conductivity of porous carbon materials and dielectric properties of composite materials with them

Uniform distribution of carbon particles in the polymer matrix was achieved through a solution method used for composite material fabrication. PS was dissolved in a stable dispersion of PCM or PCM-Br in chloroform and stirred thoroughly using US treatment. Keeping the thin films in a hood without additional heating (at 25°C) ensured slow solvent evaporation that prevented the formation of microcracking and micropores. The quality of fabricated composite materials was controlled by means of optical microscopy. Figure 4 shows optical images of PS/PCM and PS/PCM-Br in transmitted light. Dark regions in the images correspond to composite areas containing optically non-transparent PCM particles. The PS thin film, on the contrary, transmits visible light, therefore bright areas in the images correspond to polymer that are depleted of carbon filler. Samples have quite good homogeneity and uniform distribution of PCM agglomerates in the polymer matrix. As the fraction of carbon filler grows, the samples become less transparent and almost opaque at content of 10 wt%.

PCM bromination caused the increase in the electrical conductivity σ_{DC} from 0.75 ± 0.04 to 2.4 ± 0.1 S/m. The obtained values are comparable with those for other highly-porous carbon powders such as CNH [44,45]. An increase in electrical conductivity was observed previously for brominated carbon material made by polyvinylidenechloride carbonization [46] and for CNH with absorbed iodine molecules [47]. According to the literature data, the increase

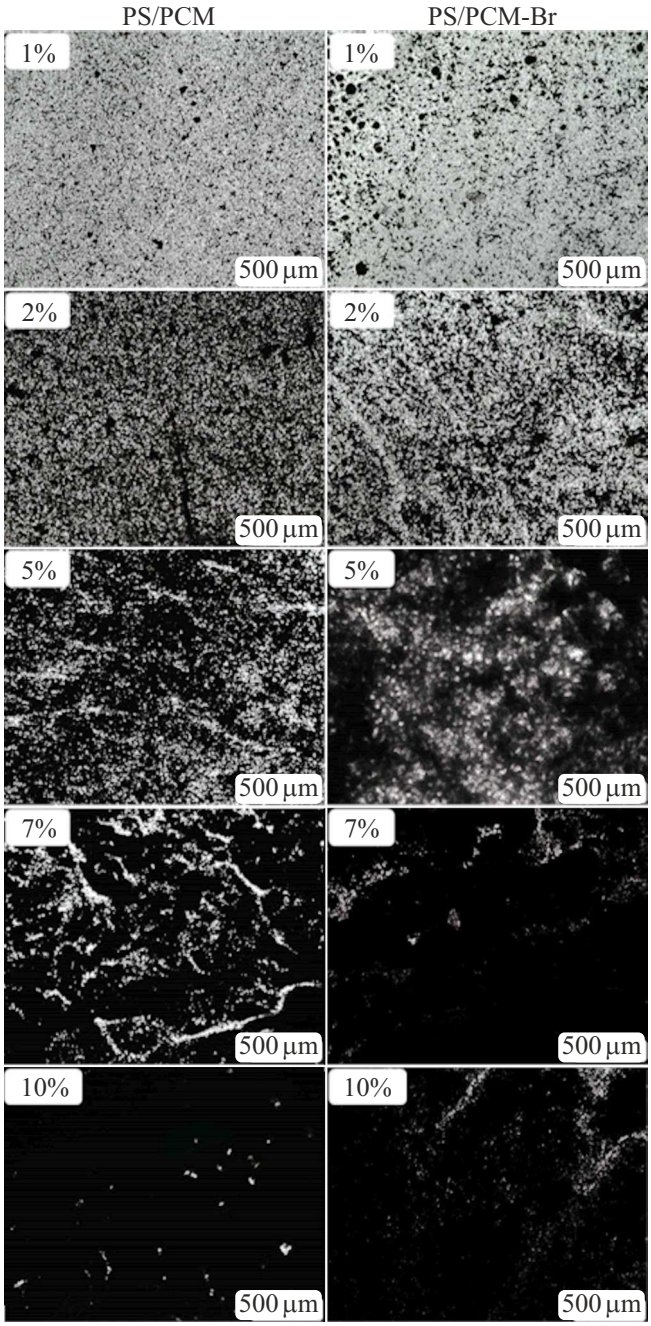

Figure 4. Optical images of composite PS/PCM and PS/PCM-Br materials with the content of filler from 1 wt% to 10 wt%.

in σ_{DC} for PCM-Br is associated with the transfer of electron density from the carbon structure surface to the intercalated Br_2 molecules that increases the concentration of positive charge carriers — holes.

Figure 5, *a*–*d* shows frequency dependences of the real ε' and the imaginary ε'' parts of the permittivity of the composite PS/PCM and PS/PCM-Br samples in the frequency range of 0.1–1.3 THz. Dielectric permittivity ε' of a PS film made without addition of carbon filler has a constant value of about 2.2, which is close to that of dense

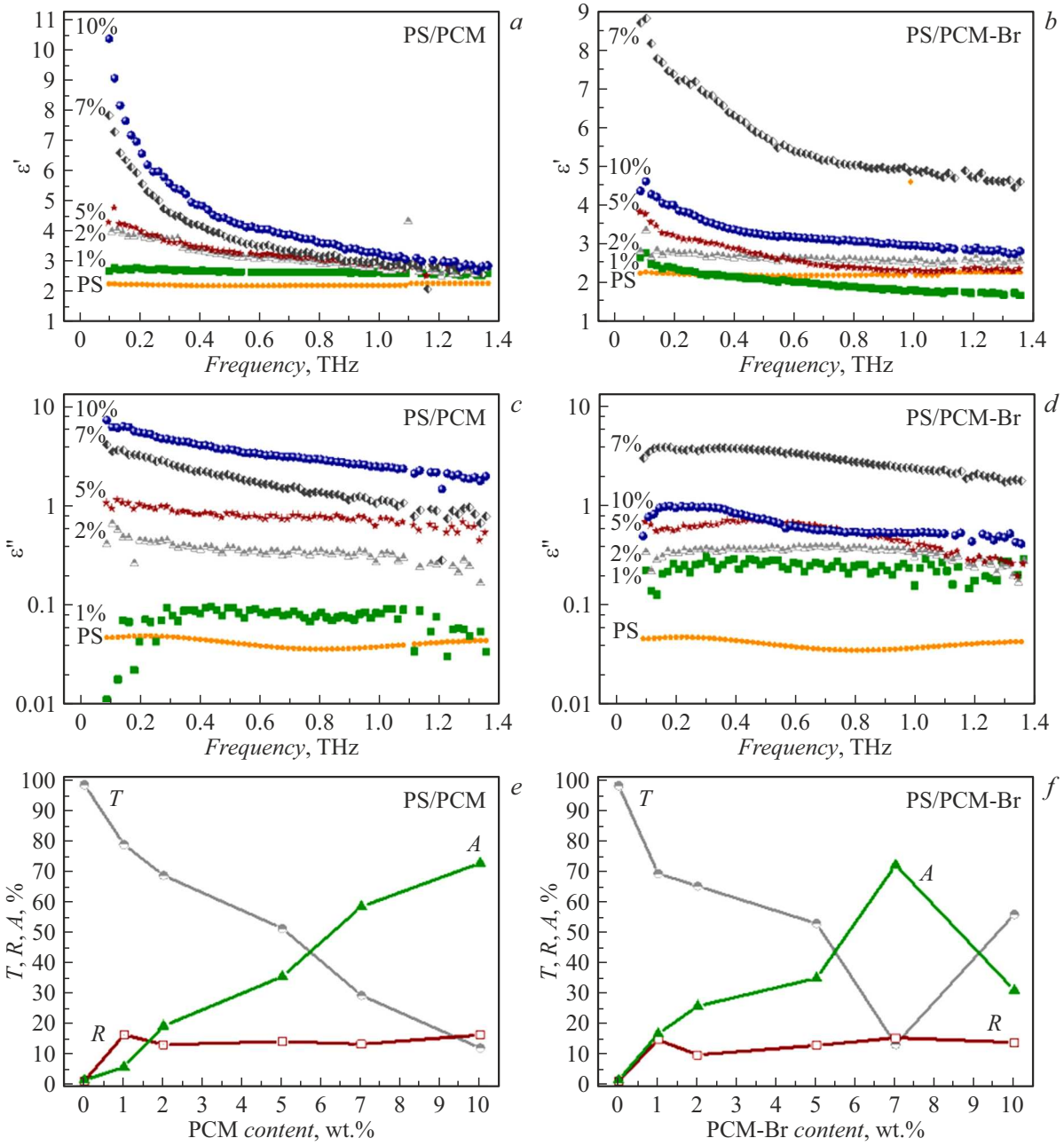

Figure 5. Electromagnetic properties of composite PS/PCM (a, c, e) and PS/PCM-Br (b, d, f) materials: real ε' (a, b) and imaginary ε'' (c, d) parts of permittivity, transmittance (T), reflectance (R) and absorbance (A) at 0.6 THz depending on the content of PCM (e) and PCM−Br (f).

bulk polystyrene [48]. Low electrical conductivity of PS ($\sigma_{DC} \sim 10^{-13}$ S/m [48]) explains low values ε'. Addition of PCM causes the increase in the permittivity (Figure 5, *a, c*). When the carbon filler concentration is 10 wt%, ε' and ε'' reach the maximum values of 3.3 and 2.4, respectively, at 1 THz.

Permittivity of PS/PCM-Br varies in a non-monotonic manner with the increase in the PCM-Br content (Figure 5, *b, d*). At 1 THz, the values of $\varepsilon'(\varepsilon'')$ increase from 1.8 to 5.0 (from 0.2 to 2.6) as the PCM-Br content grows from 1 wt% to 7 wt%. However, further increase in the PCM-Br filler concentration to 10 wt% caused the decrease in the real and imaginary parts of permittivity to 3.0 and 0.6. Such critical behavior was observed before for composite materials with CNH [10,11,49] and indicates the formation of a continuous conductive cluster chain in the polymer matrix. Thus, the effects of current flow through a composite polymer film contribute to the electromagnetic properties of the PS/PCM-Br material starting from the filler concentration of about 7 wt%. The PCM-Br concentration of 10 wt% gives rise to the decrease in ε''. This phenomenon can be associated with exclusion

of a part of composite interior from the electron transfer process when the critical filler concentration is reached [10].

Transmittance T, reflectance R and absorbance A of 100 μm-thick materials at 0.6 THz are shown in Figure 5, *e,f*. As the weight fraction of PCM increases, the composite PS/PCM materials become less transparent. Thus, the sample containing 10 wt% of the initial PCM transmits only about 11% of incident radiation. At that, absorption is the main mechanism responsible for the attenuation of THz wave, while the contribution of reflection is less than 15%.

Transparency of the PS/PCM-Br composites also decreases with the PCM-Br concentration. At 7 wt% PCM-Br, T is 12%. The contribution of absorption to the attenuation of electromagnetic radiation is higher than that for the PS/PCM series with the same weight content of carbon filler (to 7 wt%, inclusive). This could be associated with the increase in the carbon filler conductivity after bromination and with the increasing role of multiple reflection in carbon particles. Increase in the PCM-Br concentration to 10 wt% causes the increase in the fraction of transmitted radiation to 56%. This nonlinearity is associated with the appearance of conducting networks in the film with high PCM-Br concentration.

It is interesting to compare the electromagnetic properties of the prepared PS/PCM composites with the data for absorbing materials containing other carbon fillers. Composite materials consisting of polymethyl methacrylate and 0.5–2 wt% carbon onions about 100 μm in thickness transmit from 40% to 80% of incident radiation [50,51]. To achieve the same T in a 2 mm polymer plate, at least 15 wt% CNH shall be added [11]. Aerogel and carbon foam samples containing graphene [15,16], carbon nanotubes [17] and mixtures thereof [15] with thickness of 2 and 3 mm transmit less than 10% THz and 1% THz of radiation, respectively. Comparable properties were demonstrated by glass-like carbon foam [12]. Composite materials with 10 wt% PCM and 7 wt% PCM-Br 100 μm in thickness attenuate about 89 and 88% of incident radiation at 0.6 THz, thus, showing their potential for shielding coating applications.

Conclusion

PCM powder with the specific surface area of 577 m^2/g and conductivity of 0.75 S/m was synthesized by chemical deposition of acetonitrile on a CaO-doped template at 650°C. Holding PCM in saturated bromine vapor at room temperature during 4 days allowed addition of 3 at% of bromine in the form of molecular bromine and bromine atom covalently bonded to carbon atoms at the edges of defects and graphene fragments (in a ratio of 2 : 3). Bromination caused the increase in the sample conductivity to 2.4 S/m. Polystyrene and initial or brominated carbon materials were used to make composite materials with different filler concentrations of 1 wt%, 2 wt%, 5 wt%, 7 wt% and 10 wt% and their electromagnetic properties were studied in the frequency range from 0.1 THz to 1.3 THz. It was found that the addition of the studied carbon fillers caused the increase in the permittivity of the polymer samples and could provide thin films capable of attenuating the THz electromagnetic radiation significantly. Addition of a brominated carbon material increased the shielding efficiency at low filler concentrations (up to 7 wt%) due to the enhanced absorption of electromagnetic radiation by carbon particles. At high concentrations of brominated carbon filler, both conductivity and reflectance of the composite material increased. The study has demonstrated a high potential of bromine-modified PCM as functional fillers for high-performance electromagnetic polymer shields. Bromination may be used as a method for modification of other carbon nanomaterials serving as a basis for creating new conductive fillers for shielding polymer coatings with desired properties.

Funding

This study was funded by the Ministry of Science and Higher Education of the Russian Federation (project № 121031700314-5).

Acknowledgments

The authors are grateful to A.A. Zaguzina for the provision of a PCM sample, N.A. Dvurechenskaya for powder conductivity measurements and THz permittivity calculations for composite materials, and P.E. Plyusnin, PhD in chemistry, for the thermogravimetric analysis of the PCM-Br sample.

Conflict of interest

The authors declare no conflict of interest.

References

[1] D. Kobina Sam, H. Li, Y. T. Xu, Y. Cao. J. Industrial Engineering Chem., **135**, 17 (2023). DOI: 10.1016/j.jiec.2024.01.044
[2] K. Fic, A. Platek, J. Piwek, E. Frackowiak. Mater. Today, **21** (4), 437 (2018). DOI: 10.1016/j.mattod.2018.03.005
[3] L. Wang, X. Hu. Chem. — Asian J., **13** (12), 1518 (2018). DOI: 10.1002/asia.201800553
[4] A.D. Nishchakova, M.A. Grebenkina, E.V. Shlyakhova, Y.V. Shubin, K.A. Kovalenko, I.P. Asanov, Y.V. Fedoseeva, A.A. Makarova, A.V. Okotrub, L.G. Bulusheva. J. Alloys Compounds, **858**, 158259 (2021). DOI: 10.1016/j.jallcom.2020.158259
[5] G.P. Mane, S.N. Talapaneni, C. Anand, S. Varghese, H. Iwai, Q. Ji, K. Ariga, T. Mori, A. Vinu. Adv. Functional Mater., **22** (17), 3596 (2012). DOI: 10.1002/adfm.201200207
[6] M. Zacharska, L.G. Bulusheva, A.S. Lisitsyn, S. Beloshapkin, Y. Guo, A.L. Chuvilin, E.V. Shlyakhova, O.Yu. Podyacheva, J.J. Leahy, A.V. Okotrub, D.A. Bulushev. Chem. Sus. Chem., **10** (4), 720 (2017). DOI: 10.1002/cssc.201601637

[7] A.D. Nishchakova, D.A. Bulushev, S.V. Trubina, O.A. Stonkus, Y.V. Shubin, I.P. Asanov, V.V. Kriventsov, A.V. Okotrub, L.G. Bulusheva. Nanomaterials, **13** (3), 545 (2023). DOI: 10.3390/nano13030545
[8] W. Tian, H. Zhang, X. Duan, H. Sun, G. Shao, S. Wang. Adv. Functional Mater., **30** (17), 1909265 (2020). DOI: 10.1002/adfm.201909265
[9] R. Bera, S. Suin, S. Maiti, N.K. Shrivastava, B.B. Khatua. J. Appl. Polymer Sci., **132** (46), 42803 (2015). DOI: 10.1002/app.42803
[10] O.V. Sedelnikova, K.I. Baskakova, A.V. Gusel'nikov, P.E. Plyusnin, L.G. Bulusheva, A.V. Okotrub. Materials, **12** (11), 1848 (2019). DOI: 10.3390/ma12111848
[11] O.V. Sedelnikova, K.I. Baskakova, D.S. Bychanok, E.A. Maksimovskiy, L.G. Bulusheva, A.V. Okotrub. Compos. Sci. Technol., **244**, 110294 (2023). DOI: 10.1016/j.compscitech.2023.110294
[12] M. Letellier, J. Macutkevic, P. Kuzhir, J. Banys, V. Fierro, A. Celzard. Carbon, **122**, 217 (2017). DOI: 10.1016/j.carbon.2017.06.080
[13] P.P. Kuzhir, A.G. Paddubskaya, M.V. Shuba, S.A. Maksimenko, A. Celzard, V. Fierro, G. Amaral-Labat, A. Pizzi, G. Valušis, J. Macutkevic, M. Ivanov, J. Banys, S. Bistarelli, A. Cataldo, M. Mastrucci, F. Micciulla, I. Sacco, E. Stefanutti, S. Bellucci. J. Nanophoton., **6** (1), 061715 (2012). DOI: 10.1117/1.JNP.6.061715
[14] D. Bychanok, A. Plyushch, K. Piasotski, A. Paddubskaya, S. Voronovich, P. Kuzhir, S. Baturkin, A. Klochkov, E. Korovin, M. Letellier, S. Schaefer, A. Szczurek, V. Fierro, A. Celzard. Phys. Scripta, **90** (9), 94019 (2015). DOI: 10.1088/0031-8949/90/9/094019
[15] Z. Huang, H. Chen, S. Xu, L.Y. Chen, Y. Huang, Z. Ge, W. Ma, J. Liang, F. Fan, S Chang, Y. Chen. Adv. Opt. Mater., **6** (23), 1801165 (2018). DOI: 10.1002/adom.201801165
[16] P. Kumar, M. Silhavík, J. Červenka, P. Kužel. J. Phys. D: Appl. Phys., **56**, 505103 (2023). DOI: 10.1088/1361-6463/acfb1c
[17] P.A. Dróżdż, N. Xenidis, J. Campion, S. Smirnov, A. Przewłoka, A. Krajewska, M. Haras, A. Nasibulin, J. Oberhammer, D. Lioubtchenko. Appl. Mater. Today, **29**, 101684 (2022). DOI: 10.1016/j.apmt.2022.101684
[18] Y. Yamada, S. Masaki, S. Sato. J. Mater. Sci., **55** (24), 10522 (2020). DOI: 10.1007/s10853-020-04786-1
[19] L.G. Bulusheva, A.V. Okotrub, E. Flahaut, I.P. Asanov, P.N. Gevko, V.O. Koroteev, Yu.V. Fedoseeva, A. Yaya, C.P. Ewels. Chem. Mater., **24** (14), 2708 (2012). DOI: 10.1021/cm3006309
[20] J. Li, L. Vaisman, G. Marom, J.-K. Kim. Carbon, **45** (4), 744 (2007). DOI: 10.1016/j.carbon.2006.11.031
[21] K.Z. Milowska, M. Krzywiecki, M.C. Payne, D. Janas. Mater. Design, **213**, 110310 (2022). DOI: 10.1016/j.matdes.2021.110310
[22] E.V. Shlyakhova, L.G. Bulusheva, M.A. Kanygin, P.E. Plyusnin, K.A. Kovalenko, B.V. Senkovskiy, A.V. Okotrub. Phys. Status Solidi (B), **251** (12), 2607 (2014). DOI: 10.1002/pssb.201451228
[23] T. Sasa, Y. Tarahashi, T. Muraibo. Carbon, **9**, 406 (1971). DOI: 10.1016/0008-6223(71)90021-2
[24] I.V. Klimenko, A.N. Shchegolikhin, T.S. Zhuravleva. Synthetic Metals, **71**, 1773 (1995). DOI: 10.1016/0379-6779(94)03046-9
[25] N.N. Gavrilov, A.V. Okotrub, L.G. Bulusheva, O.V. Sedelnikova, I.V. Yushina, V.L. Kuznetsov. Composit. Sci. Technol., **70** (5), 719 (2010). DOI: 10.1016/j.compscitech.2009.12.026
[26] M.A. Kanygin, O.V. Sedelnikova, L.G. Bulusheva, A.V. Okotrub. Intern. J. Nanotechnol., **12** (3/4), 182 (2015). DOI: 10.1504/IJNT.2015.067203
[27] O.V. Sedelnikova, M.A. Kanygin, E.Y. Korovin, L.G. Bulusheva, V.I. Suslyaev, A.V. Okotrub. Compos. Sci. Technol., **102**, 59 (2014). DOI: 10.1016/j.compscitech.2014.07.013
[28] S.A. Sadykhov, M.R. Turbanov, Tch.A. Tchalobiev. Vysokomol. soedin., **6**, 58 (1992) (in Russian).
[29] M. Camps, A. Jebri, P. Verlaque, A. Archavlis, R. Faure. Europ. Polymer J., **29** (1), 99 (1993). DOI: 10.1016/0014-3057(93)90279-O
[30] D.A. Shirley. Phys. Rev. B, **5** (12), 4709 (1972). DOI: 10.1103/PhysRevB.5.4709
[31] A.M. Nicolson, G.F. Ross. IEEE Trans. Instrumentation and Measurement, **19** (4), 377 (1970). DOI: 10.1109/TIM.1970.4313932
[32] W.B. Weir. Proceedings of the IEEE, **62** (1), 33 (1974). DOI: 10.1109/PROC.1974.9382
[33] EM-Calculator. *Online calculator of complex dielectric permittivity and magnetic permeability in microwaves* (2022), http://em-calculator.com
[34] E.V. Shlyakhova, A.V. Okotrub, Yu.V. Fedoseeva, E.O. Fedorovskaya, E.A. Mel'gunova, M.S. Mel'gunov, V.O. Koroteev, A.A. Makarova, J. Zhou, H. Song, L.G. Bulusheva. Appl. Surf. Sci., **543**, 148565 (2021). DOI: 10.1016/j.apsusc.2020.148565
[35] Y.V. Fedoseeva, E.V. Shlyakhova, A.A. Makarova, A.V. Okotrub, L.G. Bulusheva. Nanomater., **13** (19), 2623 (2023). DOI: 10.3390/nano13192623
[36] Y.V. Fedoseeva, E.V. Shlyakhova, A.A. Vorfolomeeva, M.A. Grebenkina, V.I. Sysoev, S.G. Stolyarova, E.A. Maksimovskiy, A.A. Makarova, A.V. Okotrub, L.G. Bulusheva. Batteries, **9** (1), 45 (2023). DOI: 10.3390/batteries9010045
[37] A.C. Ferrari. Solid State Commun., **143**, 47 (2007). DOI: 10.1016/j.ssc.2007.03.052
[38] A.C. Ferrari, D.M. Basko. Nature Nanotechnol., **8** (4), 235 (2013). DOI: 10.1038/nnano.2013.46
[39] Yu.V. Fedoseeva, G.A. Pozdnyakov, A.V. Okotrub, M.A. Kanygin, Yu.V. Nastaushev, O.Y. Vilkov, L.G. Bulusheva. Appl. Surf. Sci., **385**, 464 (2016). DOI: 10.1016/j.apsusc.2016.05.120
[40] A. Supong, P.C. Bhomick, R. Karmaker, D. Sinha, U.B. Sinha. Chem. Phys. Lett., **850**, 141477 (2024). DOI: 10.1016/j.cplett.2024.141477
[41] L.G. Bulusheva, E.V. Lobiak, Yu.V. Fedoseeva, J.-Y. Mevellec, A.A. Makarova, E. Flahaut, A.V. Okotrub. Synthetic Metals, **259**, 11623 (2020). DOI: 10.1016/j.synthmet.2019.116233
[42] M.K. Rabchinskii, V.V. Sysoev, S.A. Ryzhkov, I.A. Eliseyev, D.Y. Stolyarova, G.A. Antonov, N.S. Struchkov, M. Brzhezinskaya, D.A. Kirilenko, S.I. Pavlov, M.E. Palenov, M.V. Mishin, O.E. Kvashenkina, P.G. Gabdullin, A.S. Varezhnikov, M.A. Solomatin, P.N. Brunkov. Nanomater., **12** (1), 45 (2022). DOI: 10.3390/nano12010045
[43] I.V. Klimenko, A.N. Shchegolikhin, T.S. Zhuravleva. Synthetic Metals, **86**, 2347 (1997). DOI: 10.1016/S0379-6779(97)81155-1
[44] S.M. Unni, S.N. Bhange, R. Illathvalappil, N. Mutneja, K.R. Patil, S. Kurungot. Small, **11** (3), 352 (2015). DOI: 10.1002/smll.201303892

[45] K.I. Baskakova, O.V. Sedelnikova, E.V. Lobiak, P.E. Plyusnin, L.G. Bulusheva, A.V. Okotrub. Fullerenes, Nanotubes and Carbon Nanostructures, **28** (4), 342 (2020). DOI: 10.1080/1536383X.2019.1708737
[46] J. Ozaki, I. Sunami, Y. Nishiyama. J. Phys. Chem., **94**, 3843 (1990). DOI: 10.1021/j100372a089
[47] F. Khoerunnisa, T. Fujimori, T. Itoh, H. Kanoh, T. Ohba, M. Yudasaka, S. Iijima, K. Kaneko. Chem. Phys. Lett., **501**, 485 (2011). DOI: 10.1016/j.cplett.2010.11.086
[48] A.V. Noskov, A.V. Alekseeva, O.V. Kraev, A.S. Agafonov. Khimiya i khimicheskaya tekhnologiya, **56** (2), 40 (2013) (in Russian).
[49] J. Yuan. Chinese Chem. Lett., **28** (11), 2036 (2017). DOI: 10.1016/j.cclet.2017.08.020
[50] J. Macutkevic, R. Adomavicius, A. Krotkus, D. Seliuta, G. Valusis, S. Maksimenko, P. Kuzhir, K. Batrakov, V. Kuznetsov, S. Moseenkov, O. Shenderova, A.V. Okotrub, R. Langlet, Ph. Lambin. Diamond Related Mater., **17** (7-10), 1608 (2008). DOI: 10.1016/j.diamond.2007.11.018
[51] S. Venkatachalam, K. Zeranska-Chudek, M. Zdrojek, D. Hourlier. Nano Select, **1** (5), 471 (2020). DOI: 10.1002/nano.202000067

Translated by E.Ilinskaya